

## EVALUATION OF HEAT AND MASS TRANSFER COEFFICIENTS FOR A VERTICAL TUBE ABSORBER

Muhammad Elias, N.E. Wijesundera and M.N.A. Hawlader

Department of Mechanical Engineering, National University of Singapore  
9 Engineering Drive 1, Singapore 117576.

### ABSTRACT

In this paper, a coupled heat and mass transfer model for the absorber in absorption refrigeration system is used to extract the heat and mass transfer coefficients from experimental data reported recently in literature on a vertical tube absorber. A simulation model has been developed to evaluate the effective heat and mass transfer coefficients, bulk solution to tube wall heat transfer coefficient, and interface to bulk solution heat and mass transfer coefficients. In addition, the film Nusselt number and Sherwood number are calculated and correlated with film Reynolds number. Using the experimentally determined transfer coefficients, the computer code is able to predict the distribution of the various field variables such as the temperatures of the solution and the coolant, and the concentrations in the absorber. A parametric study has been performed to investigate the effects of variation of heat and mass transfer coefficients, cooling water temperature, solution temperature and concentration with the design parameters of the absorber, such as, solution flow rate, coolant flow rate and the area of absorber. The sensitivity of the estimated heat and mass transfer coefficients to the thermo physical properties used from various sources is examined.

**Keywords:** Vapor absorption systems, heat and mass transfer coefficients, coupled model.

### 1. INTRODUCTION

Absorption refrigeration systems are becoming viable alternatives to vapor compression systems in air conditioning applications. As the absorber is the most essential component of an absorption refrigeration system, its improvement is one of the most important considerations for improving the performance. Many theoretical models have been developed and extensive experimental works have been performed to gain a better understanding of the absorption process; however, the process of absorption of water vapor in the falling film of the working fluid and the estimation of the actual heat and mass transfer coefficients from experimental data need further investigation. Moreover, design studies are needed for the improvement of the performance of practical absorbers. Islam et al. [1] has developed coupled heat and mass transfer model and performed experiments to understand and to describe the mechanism of heat and mass transfer that occurred in a tubular absorber. Miller [2] has performed the experiments on a vertical tube absorber by using lithium bromide solution as a falling film. Matsuda et al. [3] presented the results for experiments conducted on an absorber and generator in an absorption refrigeration machine made of a vertical falling-film of stainless steel column. Cosenza and Vliet [4] and Hoffman et al. [5] determined the heat transfer coefficient for tubular

absorber. Nomura et al. [6] fabricated an experimental setup to observe details of the falling film in an absorber. Tsai and Perez Blanco [7] presented that the theoretically possible maximum mass absorption rate is  $0.049 \text{ kg/m}^2\text{s}$ . Deng and Ma [8] had conducted experiment on a falling film absorber. Yoon et al. [9] conducted experiments using bare tube, bumping bare tube, floral tube, and twisted floral tube to determine the largest heat exchange area required for improving the performance of an absorber. Choudhury et al. [10] presented a physical model to analyze the absorption phenomena on the basis of various interactions between the parameters and boundary conditions involved in actual situations. Miller and Perez-Blanco [11] studied the performance of advanced (pin fin tube, grooved tube) surfaces. Miller and Keyhani [12] had presented that the concentration varies linearly in the direction of flow.

The review of the above literatures offers a scope to analyze the data of vertical tube absorber by treating the heat and mass transfer as coupled processes. In the present work, the experimental data is analyzed using coupled heat and mass transfer model [1].

### 2. MATHEMATICAL MODEL

The coupled heat and mass transfer model presented by Islam et al. [1], which embodied the theoretical

approach of the patnaik et al.[14,15], Tsai and Perez-Blanco [7] and Grossman [13], is used in the present analysis.

In Fig.1 the counter flow absorber is represented schematically. All heat and mass transfer coefficient (vapor liquid interface to solution, solution to tube wall and overall) are studied by Grossmann [13] for a laminar falling film using an analytical model. Applying the conservation laws of mass and energy to the elemental control volume shown in Fig.1, the following governing equations are obtained.

For the coolant:

$$\dot{m}_c c_c \frac{dT_c}{dA} = -U(T_s - T_c) \quad (1)$$

where, U is overall heat transfer coefficient from the bulk solution to the coolant.

The energy conservation equation for the solution is obtained by following the derivation of Tsai and Perez-Blanco [7]. The energy balance for the elemental control volume shown in Fig. 1, gives:

$$\dot{m}_s i_s + \delta \dot{m}_v i_v = (\dot{m}_s + \delta \dot{m}_s)(i_s + \delta i_s) + U(T_s - T_c)\delta A \quad (2)$$

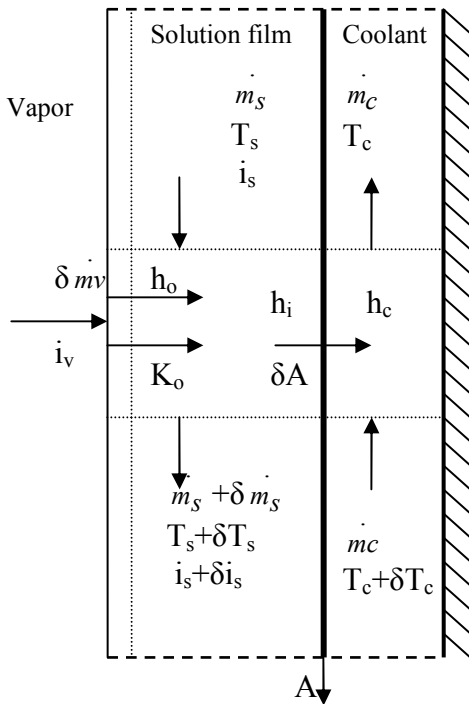


Fig 1. Physical model for counter flow absorber.

Mass balance:

$$\dot{m}_s + \delta \dot{m}_v = (\dot{m}_s + \delta \dot{m}_s) \quad (3)$$

The change in enthalpy of the solution which can be expressed in the form of

$$i_s = c'_o + c_s T_s + c'_x X_s. \quad (4)$$

It is assumed that the heat and mass transfer coefficients are suitably scaled to have a common heat transfer area dA. Using (3), the mass balance for the film can be expressed in the form:

$$\frac{d\dot{m}_s}{dA} = K_o(X_{if} - X_s) \quad (5)$$

In order to linearized (6), the following condition for the LiBr flow rate is invoked.

$$\dot{m}_l = \dot{m}_s(1 - X_s) = const. \quad (6)$$

Over the relatively small temperature range experienced by the solution, the equilibrium relation between the interface temperature and mass fraction of water at constant pressure is expressed in the linear form [15].

$$X_{if} = a - bT_{if} \quad (7)$$

By defining two new variables for the temperature difference and the mass fraction difference, the governing equations could be reduced to two coupled linear differential equations. These new variables are defined as:

$$\theta = T_s - T_c \quad \text{and} \quad \psi = a - bT_s - X_s \quad (8)$$

The temperature difference,  $\theta$  between the bulk solution and the coolant is proportional to the heat flux.  $\psi$  is the difference between the bulk solution mass fraction and the equilibrium mass fraction corresponding to local solution temperature,  $T_s$ , which is proportional to the mass flux.

The reduced equations are:

$$\frac{d\theta}{dA} = -g_3\theta + g_1\psi \quad (9)$$

$$\text{and} \quad \frac{d\psi}{dA} = bg_2\theta - g_1\beta\psi \quad (10)$$

where, the coefficients are given by:

$$g_1 = [K_{ef} i_{vs} / (\dot{m}_s c_s)](1 - c'_x / f_{i_{vs}}), \quad (11)$$

$$\frac{1}{K_{ef}} = \frac{1}{K_o} + \frac{bi_v}{h_o}, \quad (12)$$

$$g_2 = \frac{U}{\dot{m}_s c_s}, \quad (13)$$

$$g_3 = \frac{U}{\dot{m}_s c_s} - \frac{U}{\dot{m}_c c_c}, \quad (14)$$

$$\text{and } \beta = \frac{\left( b + \frac{c_s}{f_{i_{vs}}} - \frac{bc'_x}{f_{i_{vs}}} \right)}{\left( 1 - \frac{c'_x}{f_{i_{vs}}} \right)} \quad (15)$$

The overall heat transfer coefficient from the solution to the coolant can be expressed as:

$$\frac{1}{U} = \frac{1}{h_c} + \frac{1}{h_i} + \frac{\delta_w}{k_w} \quad (16)$$

And the solution of equations. (9) and (10) are obtained as:

$$\theta(A) = a_1 e^{\alpha_1 A} + a_2 e^{\alpha_2 A} \quad (17)$$

$$\text{and } \psi(A) = b_1 e^{\alpha_1 A} + b_2 e^{\alpha_2 A} \quad (18)$$

where, the roots of the characteristic equations are:

$$\alpha_1, \alpha_2 = -0.5(g_3 + \beta g_1) \pm 0.5[(g_3 + \beta g_1)^2 - 4g_1(g_3\beta - g_2b)]^{1/2} \quad (19)$$

The coefficients are given by:

$$a_1 = [\theta_0(\alpha_1 + g_1\beta) + \psi_0 g_1] / (\alpha_1 - \alpha_2) \quad (20)$$

$$a_2 = [\theta_0(\alpha_2 + g_1\beta) + \psi_0 g_1] / (\alpha_2 - \alpha_1) \quad (21)$$

$$b_1 = [\psi_0(\alpha_1 + g_3) + \theta_0 g_2 b] / (\alpha_1 - \alpha_2) \quad (22)$$

$$b_2 = [\psi_0(\alpha_2 + g_3) + \theta_0 g_2 b] / (\alpha_2 - \alpha_1) \quad (23)$$

where,  $\theta_0$  and  $\psi_0$  are the values at  $A=0$ .

The above solutions are used to 'extract' the heat and mass transfer coefficients from the experimental data reported recently in literature [2] for a vertical tube absorber. The values of the variables  $\theta$  and  $\psi$  at the inlet and outlet of the test absorber can be calculated directly from the measured temperatures of the solution and the cooling water and the water mass fractions of the solution. All other parameters such as  $c_s$ ,  $c'_x$ ,  $a$ ,  $b$  and  $i_{vs}$  are obtained from data sources. This leaves  $U$  and  $K_{ef}$  as the only unknowns in (17) and (18) which can be determined by solving these simultaneously using the Newton-Raphson method [16] or Iterative method.

It should be noted that, because  $h_o$  and  $K_o$  are embedded in  $K_{ef}$  [Eq. (12)], their individual values can be obtained only by invoking a condition such as the heat and mass transfer analogy in the form,

$$\frac{h_o}{K_o} = \left( \frac{k_s}{D_s} \right) \left( \frac{Pr}{Sc} \right)^n \quad (24)$$

where  $Pr$  and  $Sc$  are the Prandtl number and Schmidt numbers, respectively.

### 3. SIMULATION

Miller[2] presented detailed experimental data for a vertical tube absorber. For the heat and mass transfer tests, a single stainless steel absorber tube of 0.01905 meter outer diameter and 1.524 meter length, was used. The lithium bromide brine was used at a mass fraction of 0.62.

Prior to entering the solution into the absorber the strong solution is tempered by a tube in tube heat

exchanger. A coolant flows countercurrent to the falling film and supports the coupled heat and mass transfer process, as the falling film of strong solution absorbs the water vapor in the LiBr salt. The weak solution was gravity fed from the absorber to the sump tank. The weak solution is pumped from the sump and is injected into the boiler. The water is desorbed from brine by using a heater of 2.5 kW capacities in the boiler. As a result, the brine becomes stronger in LiBr salt, and the strong solution is used as the falling film in the absorber. To trim the flow of the vapor, coming from the boiler to the absorber and to tune the vapor pressure within the absorber a linear gate valve was used.

In total, 26 sets of data from Miller[2] at three different pressures are selected for the analysis. To simulate these data a computer code is written in FORTRAN. To extract the heat and mass transfer coefficients and other important variables an iterative method was used in the code. The code is able to predict and to show the variation of different temperatures, concentrations, heat flux, mass of water vapor absorbed etc. with the design parameters of the absorber, such as, solution flow rate and area of the absorber. The variation of different heat and mass transfer coefficients with the solution flow rate can also be found by using the code. Finally, the variation of Films Nusselt number and the films Sherwood number with the film Reynolds number can be observed and correlated. The code was also able to check the sensitivity of the heat and mass transfer coefficient to the enthalpy of absorption and with the index in the relation (24) of heat and mass transfer analogy.

### 4. RESULTS AND DISCUSSION

The result includes data from 26 sets of experimental runs for which the range of conditions and parameters for the model are summarized in table 1.

Table1: Range of experimental conditions and variables.

Variables	Range
$\dot{m}_s$ in (kg s <sup>-1</sup> )	1.5×10 <sup>-2</sup> -2.57×10 <sup>-2</sup>
T <sub>s in</sub> (°C)	52.7-58.1
X <sub>s in</sub>	0.3764
$\dot{m}_c$ (kg s <sup>-1</sup> )	6.25×10 <sup>-2</sup> -6.59×10 <sup>-2</sup>
T <sub>c in</sub> (°C)	34.84-35.24
I <sub>vs</sub> (kJkg <sup>-1</sup> )	2444.688-2449.346
c <sub>s</sub> (kJkg <sup>-1</sup> K <sup>-1</sup> )	1.866904-1.872599
c' <sub>x</sub> (kJkg <sup>-1</sup> )	556.751-574.1659
a	0.642-0.664
b (°C <sup>-1</sup> )	0.00485-0.00491
f	1.608726-1.613879
U (kWm <sup>-2</sup> K <sup>-1</sup> )	0.78-0.99
K <sub>ef</sub> (kgm <sup>-2</sup> s <sup>-1</sup> )	0.052-0.092

The heat transfer coefficient,  $U$  varies from 0.78-0.99 kWm<sup>-2</sup>K<sup>-1</sup> and the mass transfer coefficient  $K_{ef}$  varies from 0.052-0.092 kgm<sup>-2</sup>s<sup>-1</sup>. From literature [1], it is seen that the value of heat transfer coefficient varies

from 0.2 to 2.0  $\text{kWm}^{-2}\text{K}^{-1}$  and the mass transfer coefficient varies from 0.01 to 0.09  $\text{kgm}^{-2}\text{s}^{-1}$  for different models provided by the researcher for nearly the same range of experimental conditions.

The value of heat transfer coefficient for coolant,  $h_c$  is obtained from Dittus-Boelter correlation for flow in a tube and using that value of  $h_c$ , the value of solution to tube wall heat transfer coefficient,  $h_i$  is calculated from equation (16).

The variation of different temperatures with area is shown in Figs. 2 and 3. As expected, according to the figure 2, for a constant coolant inlet temperature, lower solution inlet temperatures lead to a reduction of the value of  $\theta$ .

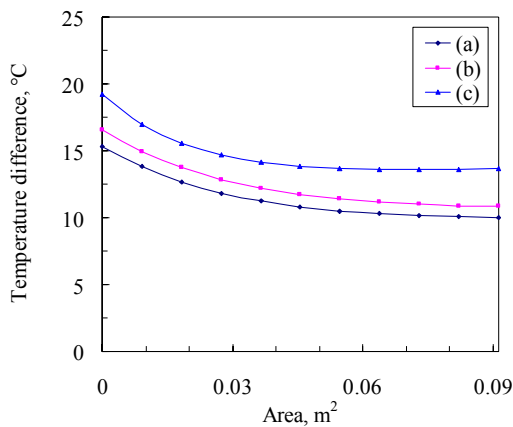


Fig.2. Variation of Temperature difference,  $\theta$  with absorber area. (a)  $T_{\text{sin}}=53.6$  °C and  $T_{\text{cin}}=35.17$  °C (b)  $T_{\text{sin}}=55.0$  °C and  $T_{\text{cin}}=35.07$  °C (c)  $T_{\text{sin}}=57.9$  °C and  $T_{\text{cin}}=34.94$  °C.

The cooling water temperature distribution was calculated by integrating equation (1) after substituting for  $(T_s - T_c)$  from equation (17).

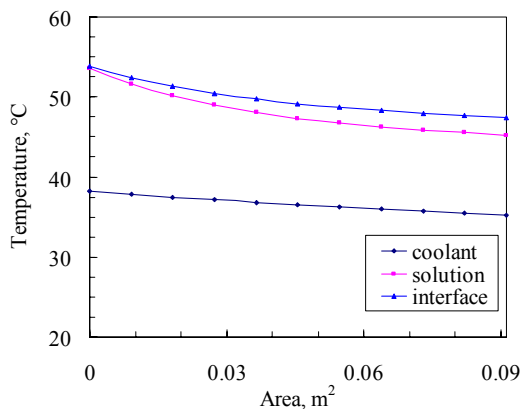


Fig.3. Variation of solution, coolant and interface temperature with area, at  $T_{\text{c,in}}=35$  °C and  $T_{\text{s,in}}=53.6$  °C.

From figure 4, it is seen that, for a constant coolant inlet temperature, with the increase of the solution inlet temperature the value of mass fraction difference is increased. From figure 4 and 5 the variation of the solution concentration with area is shown for different coolant and solution temperature.

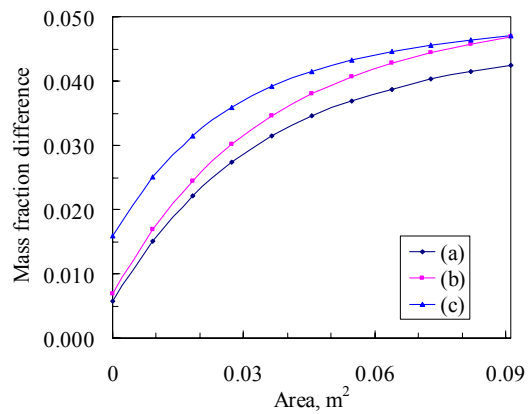


Fig. 4. Variation of mass fraction difference,  $\psi$  with area. (a)  $T_{\text{sin}}=53.6$  °C and  $T_{\text{cin}}=35.17$  °C (b)  $T_{\text{sin}}=55.0$  °C and  $T_{\text{cin}}=35.07$  °C (c)  $T_{\text{sin}}=55.5$  °C and  $T_{\text{cin}}=35.12$  °C.

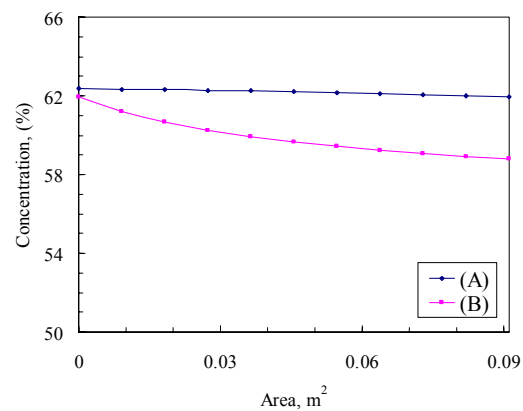


Fig. 5. Variation of concentration with area, at  $T_{\text{c,in}}=35$  °C and  $T_{\text{s,in}}=53.6$  °C. (A) for experimental solution concentration, (B) solution concentration at solution to vapor interface.

Figs. 6 and 7 show the variation of heat transfer and mass transfer coefficient with solution flow rate. From these figures, it is clear that, with the increase of solution flow rate, the heat transfer coefficient decreases; whereas the mass transfer coefficient is found maximum for a moderate solution flow rate 0.02 kg/sec for a constant solution inlet temperature and constant coolant inlet temperature. The value of mass transfer coefficient is found to be nearly 0.06  $\text{kg/m}^2\text{s}$ , which is a little bit higher than that as described by Tsai and Perez Blanco [7].

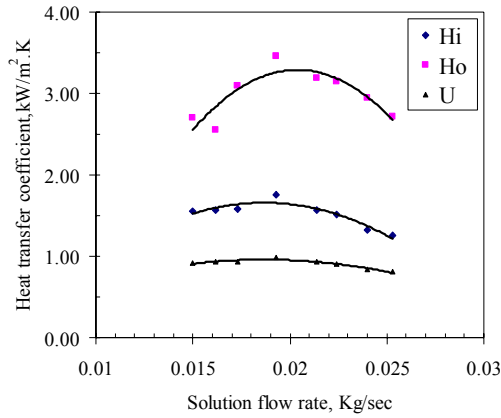


Fig. 6. Variation of overall heat transfer coefficients with solution mass flow rate at  $T_{s,in}=53.6\text{ }^{\circ}\text{C}$  and  $T_{c,in}=35\text{ }^{\circ}\text{C}$ . (U) overall, (Hi) solution to tube wall (Ho) interface to bulk solution.

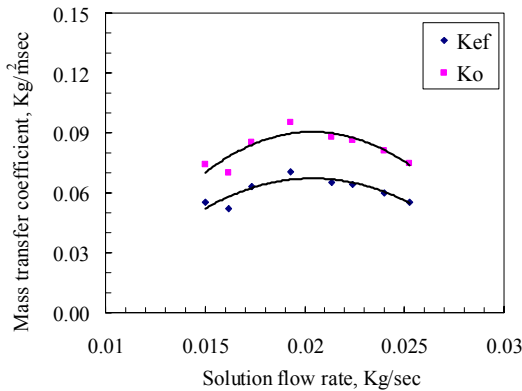


Fig. 7. Variation of mass transfer coefficient with solution mass flow rate at  $T_{s,in}=53.6\text{ }^{\circ}\text{C}$  and  $T_{c,in}=35\text{ }^{\circ}\text{C}$ . ( $K_{ef}$ ) overall and ( $K_o$ ) interface to bulk solution.

The variation of Nusselt Number, Nu (for both solution to tube wall and interface to bulk solution) with the film Reynolds Number, Re with their correlating equation can be observed from figure 8.

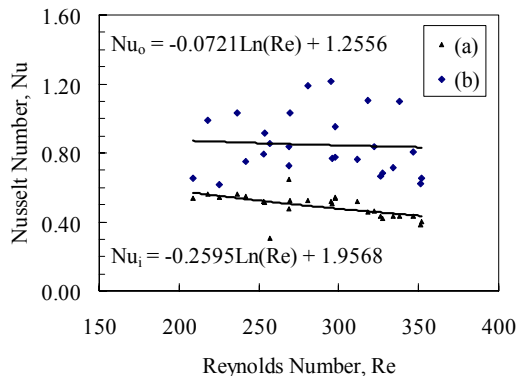


Fig. 8. Variation of film Nusselt Number (Nu) with the film Reynolds Number, Re. (a) solution to tube wall (b) interface to bulk solution.

From figure 9, the variation of film Sherwood Number, Sh with the film Reynolds Number, Re is shown with their correlating equation.

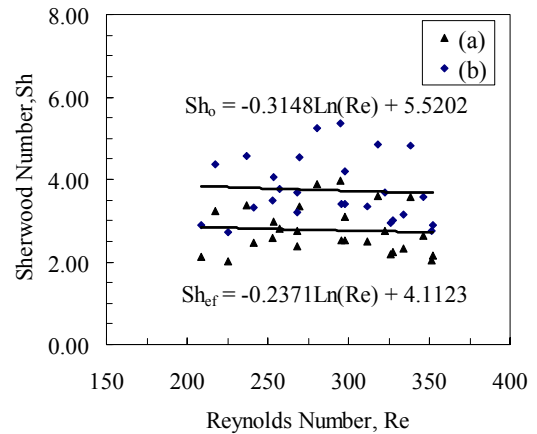


Fig. 9. Variation of film Sherwood Number, Sh with the film Reynolds Number, Re. (a) effective (b) interface to bulk solution.

In the equation of heat and mass transfer analogy value of the index, n was assigned 0.33. By varying the value of n from 0.33 to 0.4, 0.5 and 0.6, the effect was observed, which is shown in table 2. It is seen that, with the increase of n, the heat transfer coefficient from interface to bulk solution decrease; whereas the mass transfer coefficient increase up to a maximum value of  $0.2\text{ kgm}^{-2}\text{s}^{-1}$ .

Table2: Effect of index, n

n	$h_o\text{ (kWm}^{-2}\text{K}^{-1}\text{)}$	$k_o\text{ (kgm}^{-2}\text{s}^{-1}\text{)}$
0.33	2.55-5.02	0.070-0.138
0.4	2.06-4.06	0.076-0.150
0.5	1.55-3.07	0.09-0.177
0.6	1.30-2.44	0.111-0.219

The sensitivities of transfer coefficients to the variation of enthalpy of absorption is also checked. The range of all variables and transfer coefficients, as shown in table 1 are for the range of enthalpy of absorption of  $2444.6$  to  $2449.3\text{ kJkg}^{-1}$ ; and it is seen from table 3, that, if the temperature of the solution is considered as the interface temperature, the range of enthalpy of absorption does not exceed the actual range.

Table3: Effect of  $i_{vs}$

Temperature ( $^{\circ}\text{C}$ )	$i_{vs}\text{ (kJkg}^{-1}\text{)}$
Experiment temperature	2444.688-2449.346
Interface temperature	2448.306-2449.360

## 6. CONCLUSIONS

The coupled heat and mass transfer model was used to analyze the experimental data obtained from a vertical tube absorber. The heat transfer coefficient was nearly  $0.8 \text{ kWm}^{-2}\text{K}^{-1}$  and the mass transfer coefficient was nearly  $0.06 \text{ kgm}^{-2}\text{s}^{-1}$ . The variation of different field variables such as temperature difference ( $\theta$ ), mass fraction difference ( $\Psi$ ), solution and coolant temperature and solution concentration were investigated and correlation for Nusselt Number, Sherwood Number have been established as follow:

$$\text{Nu}_o = -0.0721 \text{Ln}(\text{Re}) + 1.2556$$

$$\text{Nu}_i = -0.02595 \text{Ln}(\text{Re}) + 1.9568$$

$$\text{Sh}_o = -0.3148 \text{Ln}(\text{Re}) + 5.5202$$

$$\text{Sh}_{ef} = -0.2371 \text{Ln}(\text{Re}) + 4.1123$$

The effect of enthalpy of absorption and the effect of heat and mass transfer analogy index were also analyzed.

## 5. NOMENCLATURE

Symbol	Meaning	Unit
a	constant in equilibrium relationship (7)	
$a_1$	constant in equation (17)	K
$a_2$	constant in equation (17)	K
A	absorber area	$\text{m}^2$
$A_o$	total area of absorber	$\text{m}^2$
b	constant in equilibrium relation (7)	$\text{K}^{-1}$
$b_1$	constant in equation. (18)	
$b_2$	constant in equation. (18)	
C	specific heat capacity	$\text{kJ kg}^{-1}\text{K}^{-1}$
$c_x$	Constant in expression for enthalpy	$\text{kJ kg}^{-1}$
$c_o$	Constant in expression for enthalpy	$\text{kJ kg}^{-1}$
$D_s$	Diffusivity	$\text{m}^2 \text{s}^{-1}$
F	factor in equation. (11)	
$g_1$	Constant defined in (11)	$\text{K m}^{-2}$
$g_2$	Constant defined in (13)	$\text{m}^{-2}$
$g_3$	Constant defined in (14)	$\text{m}^{-2}$
h	heat transfer coefficient	$\text{kW m}^{-2} \text{K}^{-1}$
$i_s$	Enthalpy of solution	$\text{kJ kg}^{-1}$
$i_v$	enthalpy of vapour	$\text{kJ kg}^{-1}$
$i_{vs}$	enthalpy of absorption	$\text{kJ kg}^{-1}$
$k_w$	thermal conductivity of tube wall	$\text{kW m}^{-1} \text{K}^{-1}$
$k_s$	thermal conductivity of solution	$\text{kWm}^{-1} \text{K}^{-1}$
K	mass transfer coefficient,	$\text{kg m}^{-2} \text{s}^{-1}$
$\dot{m}$	mass flow rate	$\text{kg s}^{-1}$
$\dot{M}_{abs}$	total rate of vapour absorption	$\text{kg s}^{-1}$
T	Temperature	K
U	overall heat transfer coefficient in (16)	$\text{kWm}^{-2} \text{K}^{-1}$

X	mass fraction of water in solution	
Nu	Nusselt Number	
Pr	Prandtl Number	
Re	Reynolds Number	
Sh	Sherwood Number	
$\alpha_1, \alpha_2$	roots of equation defined in (19)	$\text{m}^{-2}$
$\beta$	parameter defined in (15)	$\text{K}^{-1}$
$\delta_w$	thickness of tube wall	m
$\theta$	temperature difference defined in (8),	K
$\Psi$	mass fraction difference defined in (8)	
$\delta A$	elemental area,	$\text{m}^2$
$\delta i_s$	change of solution enthalpy	$\text{kJ kg}^{-1}$
$\delta \dot{m}_s$	change of solution mass flow rate	$\text{kg s}^{-1}$
$\delta \dot{m}_v$	vapor absorption rate	$\text{kg s}^{-1}$
c	Coolant	
s	bulk solution	
ef	effective	
ex	Exit	
i	solution to tube wall	
if	interface	
in	Inlet	
l	lithium bromide	
o	interface to bulk solution	
0	value at A=0	

## 7. REFERENCES

- [1] Islam M. R., Wijesundera N.E. and Ho J.C., Evaluation of Heat and Mass Transfer Coefficients for Falling-Films on Tubular Absorbers, *Int. J. Refrig.*, vol. 26, pp. 197-204. 2002.
- [2] Miller, W.A. The experimental analysis of aqueous lithium bromide vertical falling film absorption, PhD thesis, University of Tennessee, Knoxville, 1998
- [3] Matsuda A., Choi K.H., Hada K. and Kawamura T., Effect of pressure and concentration on performance of a vertical falling-film type of absorber and generator using lithium bromide aqueous solutions. *International Journal of Refrigeration* 17 8 (1994), pp. 538–542.
- [4] Cosenza F. and Vliet G.C., Absorption in falling water/LiBr films on horizontal tubes. *ASHRAE Transactions* 96–3379 (1990), pp. 693–701.
- [5] Hoffmann L., Greiter I., Wagner A., Weiss V. and Alefeld G. , Experimental investigation of heat transfer in a horizontal tube falling film absorber with aqueous solutions of LiBr with and without surfactants. *International Journal of Refrigeration* 19 5 (1996), pp. 331–341.
- [6] Nomura T., Nishimura N., Wei S. and Yamaguchi S., Heat and mass transfer mechanism in the absorber of water/LiBr conventional absorption refrigerator: experimental examination by visualized model.

*International Absorption Heat Pump Conference, AEA* 31 (1993), pp. 203–208.

[7] Tsai Bor-Bin and Perez-Blanco Horacio, Limits of mass transfer enhancement in lithium bromide-water absorbers by active techniques. *International Journal of Heat and Mass Transfer* 41 15 (1998), pp. 2409–2416.

[8] Deng S.M. and Ma W.B., Experimental studies on the characteristics of an absorber using LiBr/H<sub>2</sub>O solution as working fluid. *International Journal of Refrigeration* 22 (1999), pp. 293–301.

[9] Jung-In Yoon, Oh-Kyung Kwon and Choon-Geun Moon, Experimental study of heat and mass transfer on an absorber with several enhancement tubes. *Heat Transfer—Asian Research* 28 8 (1999), pp. 664–673.

[10] Choudhury S.K., Absorption of vapors into liquid films flowing over cooled horizontal tubes. *ASHRAE Trans.* Vol.99, No.2: 69-80.

[11] Miller W.A. and Perez-Blanco H., Vertical-tube aqueous LiBr falling film absorption using advanced surfaces. *International Absorption Heat Pump Conference, AES* 31 (1993), pp. 185–202.

[12] Miller W.A. and Keyhani M., The correlation of simultaneous heat and mass transfer experimental data for aqueous lithium bromide vertical falling film absorption. *Journal of Solar Energy Engineering* 123 (2001), pp. 30–42.

[13] Grossman G., Simultaneous heat and mass transfer in film absorption under laminar flow. *International Journal of Heat and Mass Transfer* 26 3 (1983), pp. 357–371.

[14] Patnaik V., Perez-Blanco H. and Ryan W.A., A simplified analytical model for the design of vertical tube absorbers. *ASHRAE Transactions* 99 2 (1993), pp. 69–80.

[15] Patnaik Vikas and Perez-Blanco Horacio. A counter flow heat-exchanger analysis for the design of falling-film absorbers. *ASME International Absorption Heat Pump Conference AES* 31 (1993), pp. 209–216.

[16] Stoecker W.F., Design of thermal systems., Graw-Hill, New York (1989).